OPEN

Transcriptome Analysis of Kidney Grafts Subjected to Normothermic Ex Vivo Perfusion Demonstrates an Enrichment of Mitochondrial Metabolism Genes

Peter Urbanellis, MD, PhD,[1,2,3] Caitriona M. McEvoy, MD, PhD,[1,2,4] Marko Škrtić, MD, PhD,[5,6] J. Moritz Kaths, MD,[1,2] Dagmar Kollmann, MD, PhD,[1] Ivan Linares, MD, PhD,[1,2,3] Sujani Ganesh, MSc,[1] Fabiola Oquendo, MD,[1] Manraj Sharma, BSc (Hons),[1] Laura Mazilescu, MD,[1,3,6] Toru Goto, MD,[1] Yuki Noguchi, MD, PhD,[1] Rohan John, MD,[7] Istvan Mucsi, MD, PhD,[2,4] Anand Ghanekar, MD, PhD,[1] Darius Bagli, MD,[8] Ana Konvalinka, MD, PhD,[1,2,3,4,7] Markus Selzner, MD,[1,2] and Lisa A. Robinson, MD[6,9]

Background. Normothermic ex vivo kidney perfusion (NEVKP) has demonstrated superior outcomes for donation-after-cardiovascular death grafts compared with static cold storage (SCS). To determine the mechanisms responsible for this, we performed an unbiased genome-wide microarray analysis. **Methods.** Kidneys from 30-kg Yorkshire pigs were subjected to 30 min of warm ischemia followed by 8 h of NEVKP or SCS, or no storage, before autotransplantation. mRNA expression was analyzed on renal biopsies on postoperative day 3. Gene set enrichment analysis was performed using hallmark gene sets, Gene Ontology, and pathway analysis. **Results.** The gene expression profile of NEVKP-stored grafts closely resembled no storage kidneys. Gene set enrichment analysis demonstrated enrichment of fatty acid metabolism and oxidative phosphorylation following NEVKP, whereas SCS-enriched gene sets were related to mitosis, cell cycle checkpoint, and reactive oxygen species ($q < 0.05$). Pathway analysis demonstrated enrichment of lipid oxidation/metabolism, the Krebs cycle, and pyruvate metabolism in NEVKP compared with SCS ($q < 0.05$). Comparison of our findings with external data sets of renal ischemia-reperfusion injury revealed that SCS-stored grafts demonstrated similar gene expression profiles to ischemia-reperfusion injury, whereas the profile of NEVKP-stored grafts resembled recovered kidneys. **Conclusions.** Increased transcripts of key mitochondrial metabolic pathways following NEVKP storage may account for improved donation-after-cardiovascular death graft function, compared with SCS, which promoted expression of genes typically perturbed during IRI.

(*Transplantation Direct* 2021;7:e719; doi: 10.1097/TXD.0000000000001157. Published online 8 July, 2021.)

Received 1 December 2020. Revision received 18 March 2021.

Accepted 20 March 2021.

[1] *Soham and Shaila Ajmera Family Transplant Centre, Toronto General Hospital, University Health Network, Toronto, ON, Canada.*

[2] *Canadian Donation and Transplantation Research Program, Edmonton, AB, Canada.*

[3] *Institute of Medical Science, University of Toronto, Toronto, ON, Canada.*

[4] *Division of Nephrology, Department of Medicine, University Health Network, Toronto, ON, Canada.*

[5] *Division of Nephrology, Department of Medicine, University of Toronto, Toronto, ON, Canada.*

[6] *Program in Cell Biology, The Hospital for Sick Children Research Institute, Toronto, ON, Canada.*

[7] *Laboratory Medicine and Pathobiology, Toronto General Hospital, University of Toronto, Toronto, ON, Canada.*

[8] *Departments of Surgery (Urology) and Physiology, The Hospital for Sick Children, Toronto, ON, Canada.*

[9] *Division of Nephrology, The Hospital for Sick Children, Toronto, ON, Canada.*

P.U. and C.M.M. contributed equally to this work.

L.A.R. and M.S. have a shared senior authorship.

The authors declare no funding or conflicts of interest.

P.U., I.M., A.G., D.B., A.K., L.A.R., and M.S. participated in research design. P.U., C.M.M., M.S., A.K, L.A.R., and M.S. participated in writing the article. P.U., C.M.M., M.S., J.M.K., D.M., I.L., S.G., F.O., M.S., L.M., T.G., Y.N., R.J., I.M., A.G., D.B., A.K, L.A.R., and M.S. participated in editing the article. P.U., M.H., D.K., I.L., S.G, and M.S. participated in performing the experiments. P.U., C.M.M., M.H., and R.J. participated in data analysis. P.U. and C.M.M. made the figures.

Supplemental digital content (SDC) is available for this article. Direct URL citations appear in the printed text, and links to the digital files are provided in the HTML text of this article on the journal's Web site (www.transplantationdirect.com).

Correspondence: Lisa A. Robinson, MD, The Hospital for Sick Children, 555 University Ave, Toronto, ON M5G 1X8, Canada. (lisa.robinson@sickkids.ca).

Correspondence: Markus Selzner, MD, General Surgery and Multi-Organ Transplant Program, Toronto General Hospital, University Health Network, University of Toronto, 585 University Ave, 11 PMB-178 Toronto, ON M5G 2N2, Canada. (markus.selzner@uhn.ca)

ISSN: 2373-8731

DOI: 10.1097/TXD.0000000000001157

Strategies to expand the kidney donation pool are critical to address the over 90 000 patients currently awaiting transplantation in the United States.[1] This has led to interest in donation-after-cardiovascular death (DCD) kidneys, which have seen an increase in their use in the United States from 7.3% in 2005 to 17.7% in 2015.[2]

DCD kidneys are associated with inferior immediate graft outcomes compared with neurological-determination-of-death donors with delayed graft function (DGF) twice as likely following DCD transplantation.[3-5] DGF has been correlated with increased incidence of acute rejection, impaired long-term function, decreased graft survival, and increased patient morbidity and mortality.[6,7] Although the cause of DGF in DCD grafts is not fully elucidated, prolonged cold ischemic time during storage has been shown to correlate with its incidence.[8]

Normothermic ex vivo kidney perfusion (NEVKP) is an emerging strategy for storage of DCD kidneys that avoids cold ischemic time. We have previously demonstrated that NEVKP, compared with static cold storage (SCS), improved function of grafts subjected to 30 min of warm ischemia mimicking DCD.[9,10] The mechanisms accounting for the improved graft function observed with NEVKP remain speculative.[11]

This study aims to identify the precise molecular mechanisms associated with the improvement in DCD graft function following NEVKP compared with SCS. To address this, we conducted an unbiased examination of the differences in the transcriptional expression of these grafts following storage.

MATERIALS AND METHODS

Expanded details are provided in the Supplemental Methods (SDC, http://links.lww.com/TXD/A326).

Experimental Design Overview

Transcriptional profiling using microarray was performed in a porcine DCD autotransplantation model at postoperative day (POD) 3 using 3 groups: 8-h NEVKP, 8-h SCS, and no storage (NS) (Figure 1A). NS kidney was included to mimic allograft injury in a living donor transplant. An overview of the workflow from graft biopsy, RNA extraction, and microarray analysis is depicted in Figure 1B.

Animals and Surgical Procedure

Male Yorkshire pigs weighing 30 kg were obtained from Caughell farms (Fingal, ON). The husbandry and experimental protocols were approved by our institutional research ethics board. All care provided to these animals followed the "Principles of Laboratory Animal Care" created by the National Society for Medical Research and the "Guide for the Care of Laboratory Animals" produced by the National Institutes of Health. Water and food were provided ad libitum while animals were housed in species-adapted housing.

Kidney retrieval and transplantation protocols and postoperative care were previously reported by our group and are available in the Supplemental Methods (SDC, http://links.lww.com/TXD/A326).

Kidney Storage Groups

The NEVKP setup of our group has been previously reported in detail.[9,12] Briefly, grafts were continuously perfused with a converted S3 heart-lung machine with an erythrocyte-based perfusate that mimicked physiological conditions with the addition of oxygen and nutrients at normal body temperatures. Details are available in the Supplemental Methods (SDC, http://links.lww.com/TXD/A326), as are the protocols

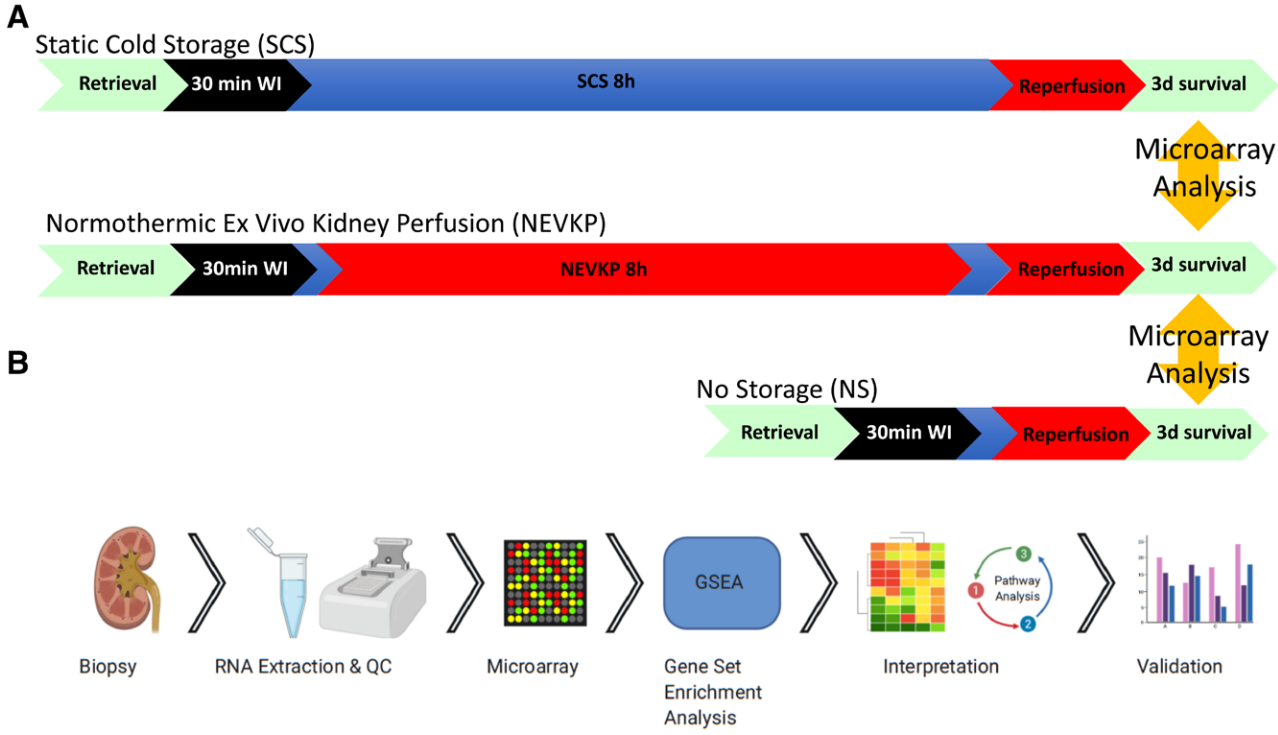

FIGURE 1. Study design. A, Experimental groups. All kidneys were subjected to 30 min of warm ischemia before procurement followed by either 8 h of SCS (SCS group), 8 h of NEVKP (NEVKP group), or were immediately reimplanted after cold flushing (NS group). Wedge kidney biopsies were taken at POD3 and placed in RNAlater; n = 3 per group. B, Microarray analysis workflow overview. GSEA, gene set enrichment analysis; NEVKP, normothermic ex vivo kidney perfusion; POD, postoperative day; SCS, static cold storage; WI, warm ischemia.

for the previously described in SCS and NS groups.[10] Grafts with NEVKP and SCS were stored for 8 h, whereas grafts in the NS group were immediately reimplanted after flushing.

RNA Extraction and Microarray

With the animal under anesthesia, wedge sections measuring 0.5 cm^3 were taken under sterile conditions from the superior pole of the graft on POD3 and placed in 1 mL RNAlater solution (Sigma-Aldrich, Oakville, ON) at 4°C for up to 1 mo. RNAlater solution was then removed and discarded as the tissue was placed in a −80°C freezer for processing later. RNA was extracted from tissue (n = 3 per group) using the RNeasy Kit (Qiagen, Toronto, ON) as per manufacturer's instruction, and the quality was tested with a spectrophotometer. RNA quality was confirmed using a Bioanalyzer 2100 with the RNA6000 Nano LapChip Kit (*both* Agilent Technologies Canada Inc., Mississauga, ON). Samples were deemed adequate for microarray analysis with an RNA integrity number ≥7. Transcriptome profiling of extracted RNA was performed using the GeneChip Porcine Gene 1.0 ST Array examining 19 212 genes.

Microarray Analysis

Microarray analysis was performed using packages sourced from the Bioconductor repository and implemented in the R statistical environment.[13] Background correction and robust multiarray-based $\log_2$ normalization[14] were performed using "oligo" (V.1.48).[15] Boxplots of the raw intensity data were inspected before and after normalization (Figure S1, SDC, http://links.lww.com/TXD/A326). Following gene-level summarization,[16] the resultant expression set underwent interquartile range based filtering (variance cutoff 0.25) using "genefilter" (V.1.66.0)[17] to exclude probes exhibiting little variability in expression across all samples. Differential expression (DE) testing was performed on the filtered data set (7592 probes) using "limma" (V.3.34.14).[18]

Initial probe-to-gene annotation for the entire data set was performed with the relevant Affymetrix annotation file.[19] Following this, we noted that many of the main probes (5437) lacked a gene assignment and remained annotated with transcript IDs (NCBI/RefSeq or Ensembl ID), sequence ID (GenBank), or genomic coordinates (GenScan). These were interrogated manually and assigned to their respective genes in the current reference genome (Ensembl SScrofa 11.1). Human orthologous of porcine genes were identified from the Ensembl genome browser (http://useast.ensembl.org/index.html) and the HGNC ortholog prediction tool (https://www.genenames.org/tools/hcop/). Downstream functional analyses of this data set were performed using the human genome identifiers.

Gene Ontology, Gene Set Enrichment Analysis, and Enrichment Map

We used Gene Ontology (GO) analysis and gene set enrichment analysis (GSEA) to explore the molecular associations of SCS- and NEVKP-treated kidneys, respectively.

GO analysis for lists of DE genes was conducted using g:Profiler.[20] We examined the expression set relating to the 2 phenotypes of interest (NEVKP and SCS) for significantly enriched (false discovery rate-adjusted P value $[q] < 0.05$) GO terms, pathway gene sets (reference gene sets available from http://baderlab.org/GeneSets), and the hallmark gene sets of the Molecular Signatures Database (MSigDB) (http://software.broadinstitute.org/gsea/msigdb/index.jsp) using GSEA.[21] The "EnrichmentMap" plug-in of Cytoscape was used to create an enrichment map of the GSEA results, depicting the overlap among pathways, with similar biological processes grouped together as subnetworks.[22-24] Gene sets and pathways with $q < 0.05$ were used as input, and a conservative overlap coefficient (0.5) was used to build the enrichment map. The "AutoAnnotate" plug-in identified clusters in an automated manner, visually annotating them with a summary label.[25]

Analysis of External Data Sets

GSEA ranked the genes in our data set based on a measure of each gene's DE with respect to the 2 phenotypes (NEVKP and SCS). PCA was used to confirm that these rankings accounted for the variability in our data set. We explored the context of our findings in relevant external data sets by examining for overlap between the GSEA-ranked gene list and DE transcripts in relevant published studies.

Liu et al[26] used RNA-seq at multiple time points (ranging from 2 h to 12 mo post-IRI) to profile the temporal-specific alterations in gene expression following bilateral severe IRI and consequent progression to chronic kidney disease (CKD) in mouse kidneys. We accessed the gene expression omnibus-deposited expression values for all samples (GSE98622) to examine expression of our top GSEA-ranked genes in their data set, focusing on the time points most closely matched to our experimental design. Finally, the list of genes DE in these mice when compared with both sham-operated and age-matched controls is supplied in the supplemental material. We examined expression of these genes in our data set in NEVKP and SCS groups, respectively, with particular focus on time points most closely matched to our experimental design.

Tran et al[27] studied the gene expression profiles of mice subjected to a sepsis-induced acute kidney injury (AKI) induced by lipopolysaccharide. All mice received fluid resuscitation after developing AKI; some then recovered baseline renal function, whereas others did not. We downloaded the raw data files for this study (GSE30576-GPL8759) and after preprocessing and Log_2 normalization (limma V.3.34.14),[18] generated an expression data set for all animals (baseline, AKI, recovered, and nonrecovered). We extracted the values for the genes corresponding to our GSEA-ranked genes (150 NEVKP, 150 SCS). In total, 173 were represented in the murine data set. The expression profiles of these genes across all samples were plotted using a heatmap (pheatmap V.1.0.12) with unsupervised hierarchical clustering of genes and samples.

Internal Validation With Quantitative Reverse-Transcriptase Polymerase Chain Reaction

The cDNAs encoding prominin1 *(prom1)*, retinol-binding protein 4 *(rbp4)*, polypeptide *N*-acetylgalactosaminyltransferase *(galnt11)*, uromodulin *(umod)*, mitochondrial pyruvate carrier-2 *(mpc2)*, and TATA-binding protein 1 *(tbp1)* were amplified from RNA extracted from a different section of the same kidneys using Superscript VILO Master Mix (ThermoFisher) with the appropriate primer pairs (Table S1, SDC, http://links.lww.com/TXD/A326). Equal amounts of cDNA for each sample were added to a prepared master-mix (SSoFast Evagreen Supermix; Bio-Rad, Hercules, CA). Quantitative reverse-transcriptase polymerase chain reactions were performed on an AB StepOnePlus Real-Time Polymerase Chain Reaction system

(Applied Biosystems, Foster City, CA) at an annealing temperature of 56°C. The relative abundance of a transcript was represented by the threshold cycle of amplification (C_T), which is inversely correlated to the amount of target RNA/cDNA being amplified. To normalize for equal amounts of cDNA, the *tbp1* gene was assayed as done previously in porcine tissue.[28] The comparative C_T method was calculated per manufacturer's instructions with fold-change relative to the SCS condition. Significance for validation of specific transcripts was performed with a 2-tailed *t* test based on the delta C_T measurements between the transcript of interest subtracted from the reference transcript *tbp1*.

RESULTS

NEVKP Improves Posttransplantation Renal Function of Grafts Injured by 30 Min of Warm Ischemia

We leveraged 3 previously reported groups of animals: NS, NEVKP, and SCS (Figure S2, SDC, http://links.lww.com/TXD/A326), using 3 animals per group for transcriptomic analysis.[9,10] The renal function of this cohort is shown in Figure S3 (SDC, http://links.lww.com/TXD/A326). POD3 serum creatinine was elevated in the SCS group compared with the NEVKP group (12.2 ± 1.1 mg/dL [1078.7 ± 97.3 μmol/L] versus 3.5 ± 1.7 mg/dL [309.5 ± 150.3 μmol/L], $P = 0.002$), and compared with the NS group (4.1 ± 1.5 mg/dL [362.5 ± 132.6 μmol/L], $P = 0.001$). There was no difference at this time point between NEVKP and NS kidneys ($P = 0.63$).

The Profile of NEVKP-treated Kidneys Resembles That of No Storage Kidneys

In our experimental design, the NS group is spared any additional ischemic damage as grafts are immediately retransplanted without storage. We hypothesized that kidneys subjected to NEVKP would more closely resemble the profile of NS kidneys than kidneys subjected to SCS. To study this, we performed an analysis for DE genes between NS and SCS and additionally, between NS and NEVKP. A total of 304 probes corresponding to 290 annotated genes were DE ($q < 0.05$) between NS and SCS (Table S2, SDC, http://links.lww.com/TXD/A326). Strikingly, no genes were DE between NS and NEVKP, even with a more lenient false discovery rate of 0.2 (Figure 2). We next explored the significantly enriched ($q < 0.05$) pathways associated with the DE genes between NS and SCS. Pathways whose members had increased expression in SCS included those related to the inflammatory response (interleukin [IL]-4 and IL-13 signaling and beta-catenin signaling in T cells), oxidative stress, the Notch developmental signaling pathway, and organization of the extracellular matrix (ECM) (Table S3, SDC, http://links.lww.com/TXD/A326).

The pathways with reduced representation in SCS, as compared with NS, reflected key pathways of normal renal metabolism (eg, fatty acid β-oxidation) and tubular function (eg, transport of small molecules and SLC-mediated transmembrane transport) (Table S4, SDC, http://links.lww.com/TXD/A326).

NEVKP Leads to Enrichment in Metabolic Genes and SCS to Cell Cycle and Profibrotic Genes

Next, we explored the key differences between NEVKP and SCS in our data set. We identified 12 genes as being DE between these conditions, 6 with increased expression in NEVKP, and 6 with increased expression in SCS ($q < 0.15$) (Table 1). Some of these genes were particularly interesting. For example, *umod* (increased in NEVKP) is an abundantly expressed kidney-specific gene whose downregulation has been linked to several kidney diseases.[29] *Cdkl2* (increased in NEVKP) is a cell cycle-related gene, and cell cycle is commonly disrupted following IRI.[30] However, these genes as a group were not enriched in specific processes/pathways. We wondered if small but congruent changes in the expression of related genes (gene sets) might be present in our data set, and although changes in individual genes might not reach statistical significance, concordant changes in multiple pathway members might enable us to pinpoint the important biological processes that are involved.[21] Consequently, we used GSEA, a widely used tool that evaluates microarray data by querying sets of related genes.[21] GSEA revealed that NEVKP was significantly enriched for gene sets related to interferon (IFN)-α and IFN-γ signaling in comparison with SCS ($q < 0.001$) (Figure 3A; Table S5, SDC, http://links.lww.com/TXD/A326). Interestingly, oxidative phosphorylation ($q < 0.001$) and fatty acid metabolism ($q = 0.003$) were also significantly enriched in NEVKP compared with SCS, reinforcing our earlier observation that the profile of NEVKP-treated kidneys is more analogous to the NS group than to SCS. Meanwhile, gene sets related to cell cycle checkpoint ($q < 0.001$), including targets of the E2F transcription factors ($q = 0.017$), known to transcriptionally regulate many cell cycle genes, were increased in SCS, as were "reactive oxygen species" genes ($q = 0.024$) (Figure 3A; Table S6, SDC, http://links.lww.com/TXD/A326).[31,32] GSEA returns ranked lists of genes whose expression most highly correlates with the stated phenotypes represented in the data set. Close inspection of the expression of the top 100 genes from this ranked list (50 genes with expression correlating highly with NEVKP phenotype and 50 SCS-correlating genes, respectively) using an unsupervised clustering analysis confirmed complete and clear separation between NEVKP and SCS (Figure 3B). Importantly, 7 of 12 genes identified as DE between NEVKP and SCS in the first analysis were also among these 100 genes (red lines, Figure 3B). We next examined the top 1000 genes (top 500 NEVKP-correlating and top 500 SCS-correlating, respectively) using principal component analysis (PCA), which confirmed complete separation of the experimental groups along the first principal component, and over 80% of the variability of the data set described by the first 2 principal components (Figure 3C). Confident that this list captured the major differences in expression between SCS and NEVKP, GSEA-ranked genes were used for downstream functional analyses (Table S7, SDC, http://links.lww.com/TXD/A326).

Functional Annotation of NEVKP- and SCS-treated Kidneys

We examined the functional annotation of the gene set enrichment results and used the output from GSEA to examine the GO terms and biological pathways significantly enriched in NEVKP and SCS, respectively. To overcome the redundancy encountered with GO terms and to aid interpretation of our overall findings, we used Enrichment Maps to create a network-based representation of our results.[33] The most prominent cluster of significantly enriched terms in NEVKP related to fatty acid metabolism thought to be the principal

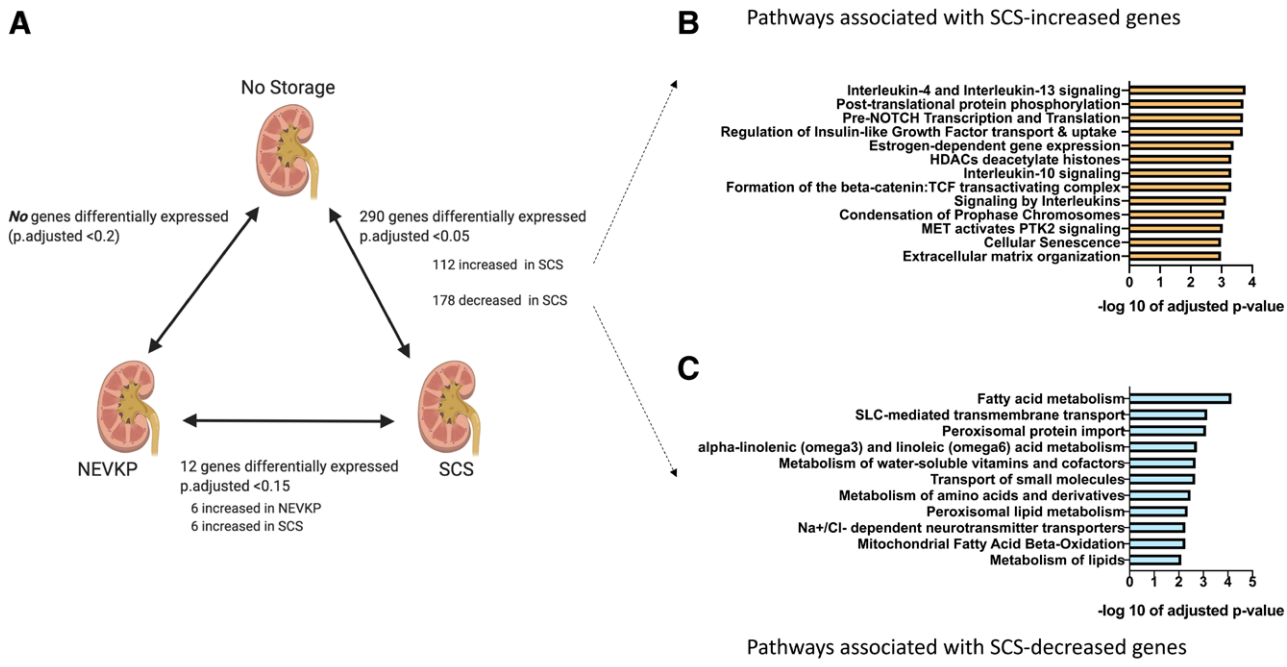

FIGURE 2. The profile of NEVKP-treated kidneys more closely resembles that of NS kidneys than SCS-treated kidneys. A, Schematic depicting the results of differential expression analysis between the NS, SCS-, and NEVKP-treated kidneys. Representative significantly enriched ($q<0.05$) pathways increased (B) and decreased (C) in SCS in comparison with NS kidneys. HDAC, histone deacetylases; MET, mesenchymal-epithelial transition; NEVKP, normothermic ex vivo kidney perfusion; NS, no storage; PTK2, protein tyrosine kinase 2; SCS, static cold storage; SLC, solute carriers; TCF, T-cell factor.

means by which proximal tubular epithelial cells generate ATP (Figure 4A).[34] Similarly, other clusters featured terms related to other critical aspects of cellular metabolism such as the tricarboxylic acid (TCA) cycle, oxidative phosphorylation, amino acid synthesis, and ATPase binding. Processes related to solute and small molecule transport (important functions of the kidney) were also significantly enriched in NEVKP. Finally, pathways related to IFN signaling, chemokine signaling, binding, and chemotaxis were enriched in NEVKP, indicating initiation of inflammatory responses in the kidney's recovery from ischemic injury.

In contrast, in SCS, the most prominent clusters recapitulated changes in the transcriptional profile associated with IRI, namely terms related to ribosome assembly, altered transcription and translation, altered protein targeting, nuclear division and DNA replication, histone modification, and cell cycle checkpoint and regulation (Figure 4B). Furthermore, additional processes linked with wound healing and fibrosis also appear, namely ECM organization, integrin signaling, and cadherin binding. Full details of enriched GO terms and pathways are shown in Tables S8 and S9 (SDC, http://links.lww.com/TXD/A326).

Validation of Findings in Relevant External Data Sets

We hypothesized that genes whose expression was modified by NEVKP in the aftermath of IRI in comparison with

TABLE 1.

Differential expression of genes perturbed in NEVKP with respect to SCS-stored grafts at postoperative day 3

HGNC ID	Gene name	Log2 fold-change (in NEVKP)	*P*	*q* Value
SLC5A8	Solute carrier family 5 member 8	2.89593924	0.00024307	0.14195333
UMOD	Uromodulin	2.37964949	0.0001311	0.12441538
ETNPPL	Ethanolamine-phosphate phospho-lyase	1.70703808	0.00029592	0.16047112
UBD	Ubiquitin D	1.46924339	5.48E-05	0.06937198
CDKL2	Cyclin-dependent kinase like 2	1.34980967	0.00011899	0.12441538
CAMK1D	Calcium/calmodulin-dependent protein kinase ID	1.23263853	0.00022519	0.14195333
REG3G	Regenerating islet-derived 3 gamma	−1.5063893	0.0002029	0.14003603
RNF39	Ring finger protein 39	−1.5235889	0.00015485	0.13062442
RBP4	Retinol-binding protein 4	−1.6585113	2.28E−05	0.03460853
SERPINA3	Serpin A3-8	−1.6687894	1.94E−05	0.03460853
RNU6-20P	U6 spliceosomal RNA	−1.8709582	1.22E−05	0.03088562
AKR1C1	Aldo-keto reductase family 1, member C1	−2.302107	9.92E−06	0.03088562

NEVKP, normothermic ex vivo kidney perfusion; SCS, static cold storage.

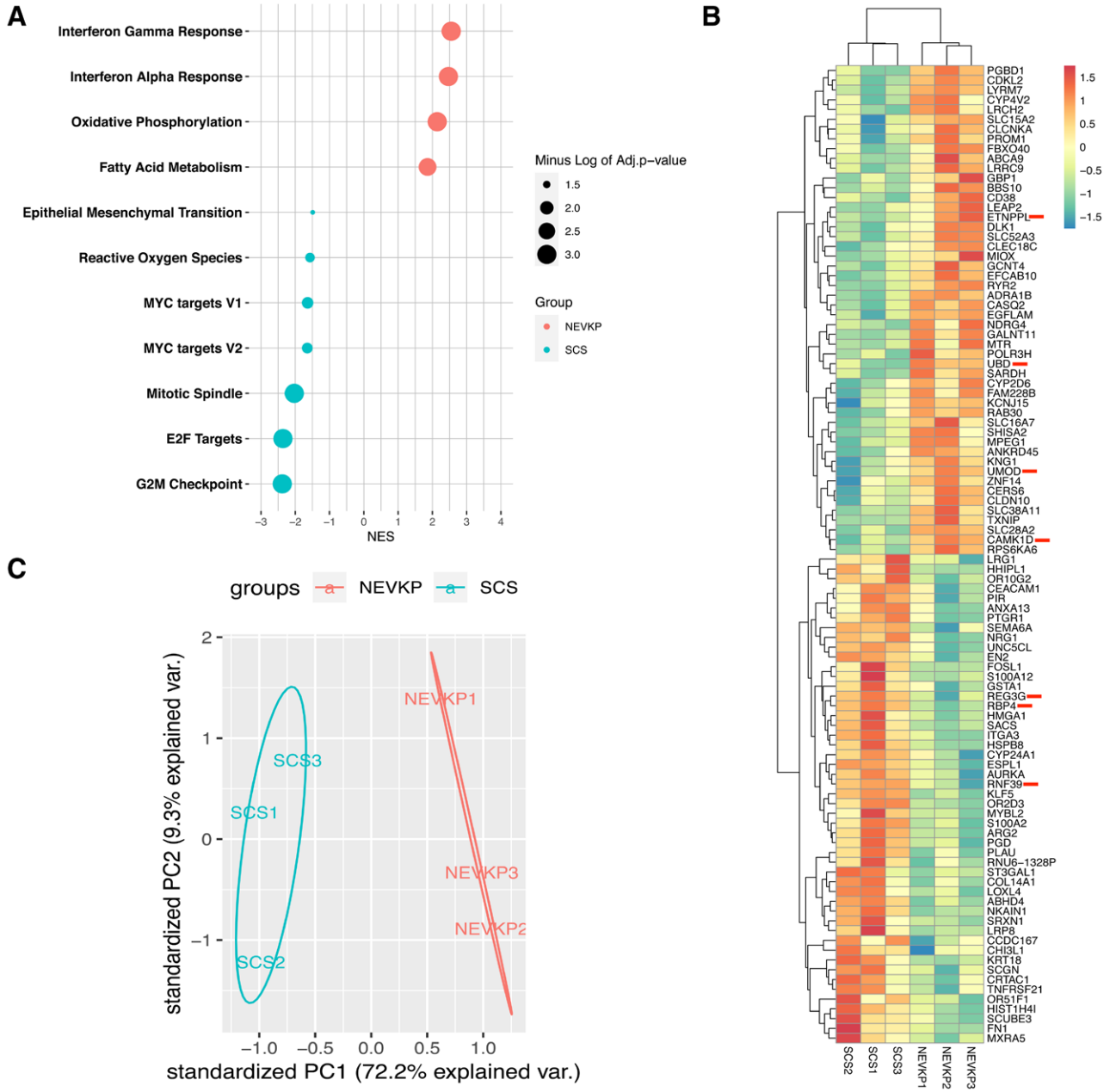

FIGURE 3. GSEA reveals the key gene sets between NEVKP- and SCS-treated kidneys. A, Significantly enriched Hallmark gene sets in NEVKP (top, red), and SCS (bottom, turquoise). NES is plotted on the x-axis. Enriched gene sets are plotted on the y-axis. Node size depicts the negative log of *q* value. B, Heatmap showing expression of top 100 genes (50 most correlated with NEVKP, and 50 most correlated with SCS) identified by GSEA with unsupervised hierarchical clustering analysis. Columns represent the samples (annotated at the bottom) and rows represent the genes, with relative expression of each gene across all samples demonstrated by pseudocolor scale ranging from –2 (green = lower expression) to +2 (red = higher expression). Red lines depict the overlap of 7 of 12 DE genes among the top GSEA-ranked genes (C). PC analysis of the top 1000 GSEA-identified genes (500 most NEVKP-correlating, and 500 most SCS-correlating) shows separation along the first PC. The percent of the variability described by PCs 1 and 2 is indicated on the x-axis and y-axis, respectively. DE, differential expression; GSEA, gene set enrichment analysis; NES, Normalized Enrichment Score; NEVKP, normothermic ex vivo kidney perfusion; PC, principal component; SCS, static cold storage.

SCS would also emerge as significantly perturbed in other data sets of IRI or AKI. Liu et al[26] performed bulk RNA sequencing to characterize the time-dependent gene expression changes in murine kidneys following bilateral IRI in comparison with sham-operated kidneys and age-matched controls. They identified 7 modules comprising 1927 genes as being DE over time, the majority of which had increased expression following IRI. Out of our 1000 GSEA-ranked genes, 185 featured among the DE genes of the Liu data set. The expression of these genes in the Liu data set at the early time points (24 h to 7 d) following IRI was examined using PCA, which clearly segregated the sham, early injury (24–72 h), and recovering injury (7 d) groups, underscoring the extent to which our data set recapitulates the gene expression profile of IRI (Figure 5A). Four of these genes were independently validated as described next. Next, we

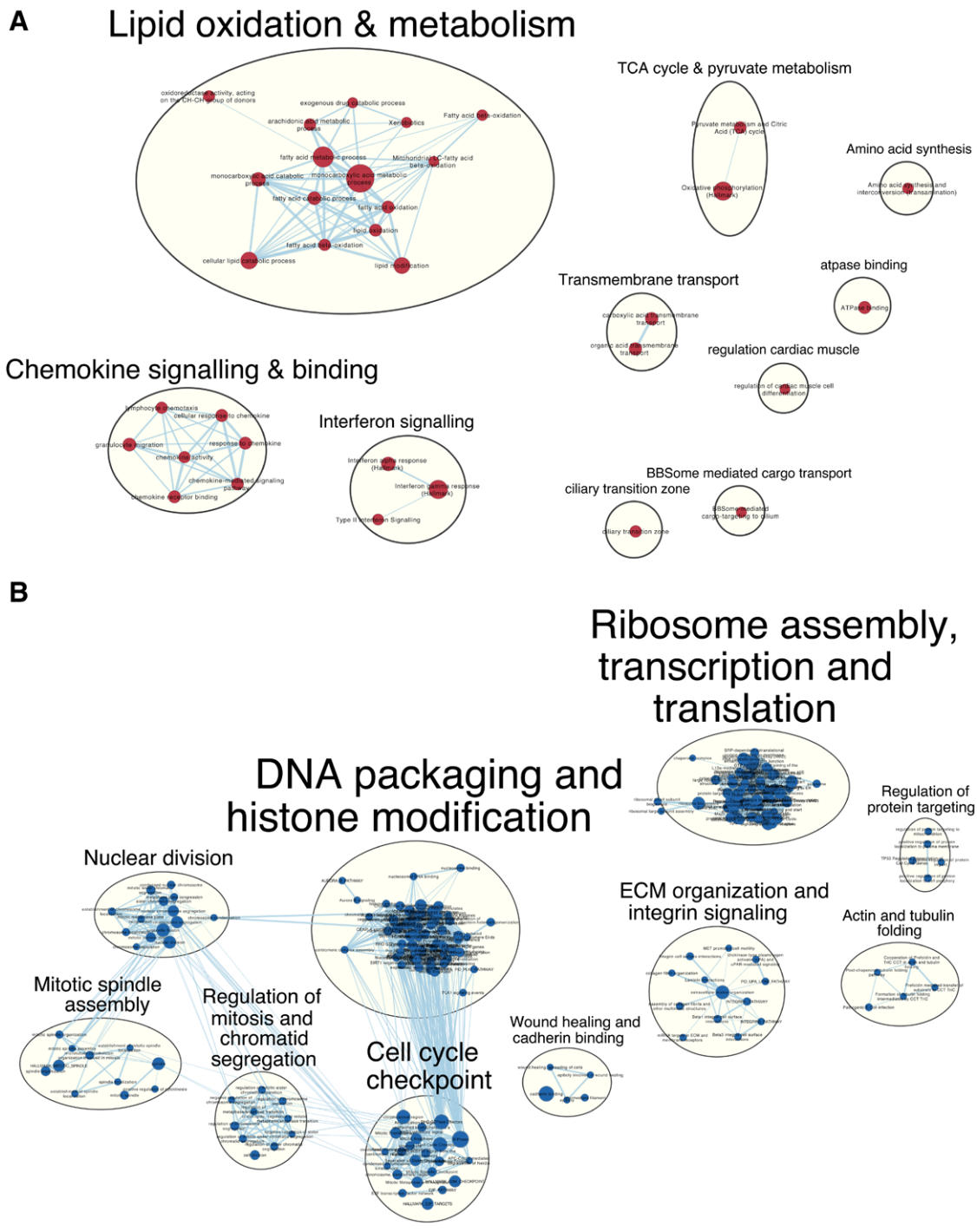

FIGURE 4. Functional annotation of NEVKP- and SCS-treated kidneys. Enrichment maps of enriched GO terms and pathways in NEVKP (A) and SCS (B) treated kidneys. Each node represents a significantly enriched (q value <0.05) GO term or pathway. The edges (blue lines) denote overlapping genes between 2 pathways, with edge thickness indicating a greater number of overlapping genes, determined by the similarity coefficient. Node size denotes gene set size. Visual summaries of clustered nodes are shown, depicting frequently occurring terms within the node cluster. GO, Gene Ontology; NEVKP, normothermic ex vivo kidney perfusion; SCS, static cold storage; TCA, tricarboxylic acid.

focused specifically on the genes with reduced expression following IRI and demonstrate that the majority (29/34 genes) also have reduced expression in SCS compared with NEVKP in our data set, whereas NEVKP-treated kidneys mirror the expression profiles of sham-operated kidneys (Figure 5B). We next examined the expression of the DE genes from the Liu study in our data set. Interestingly, genes whose expression was significantly modified in this external study of IRI, also correctly segregated the 3 groups in our study (NEVKP, SCS, and NS)—emphasizing its validity, and importantly, the profile of NEVKP-treated kidneys is clearly different from SCS-treated kidneys (Figure 5C). Finally, we examined the GSEA-ranked genes in a model of sepsis-induced AKI. This study included mice at baseline, with AKI, and, additionally, mice that recovered or did not recover renal function after fluid resuscitation.[27] We examined the expression profiles

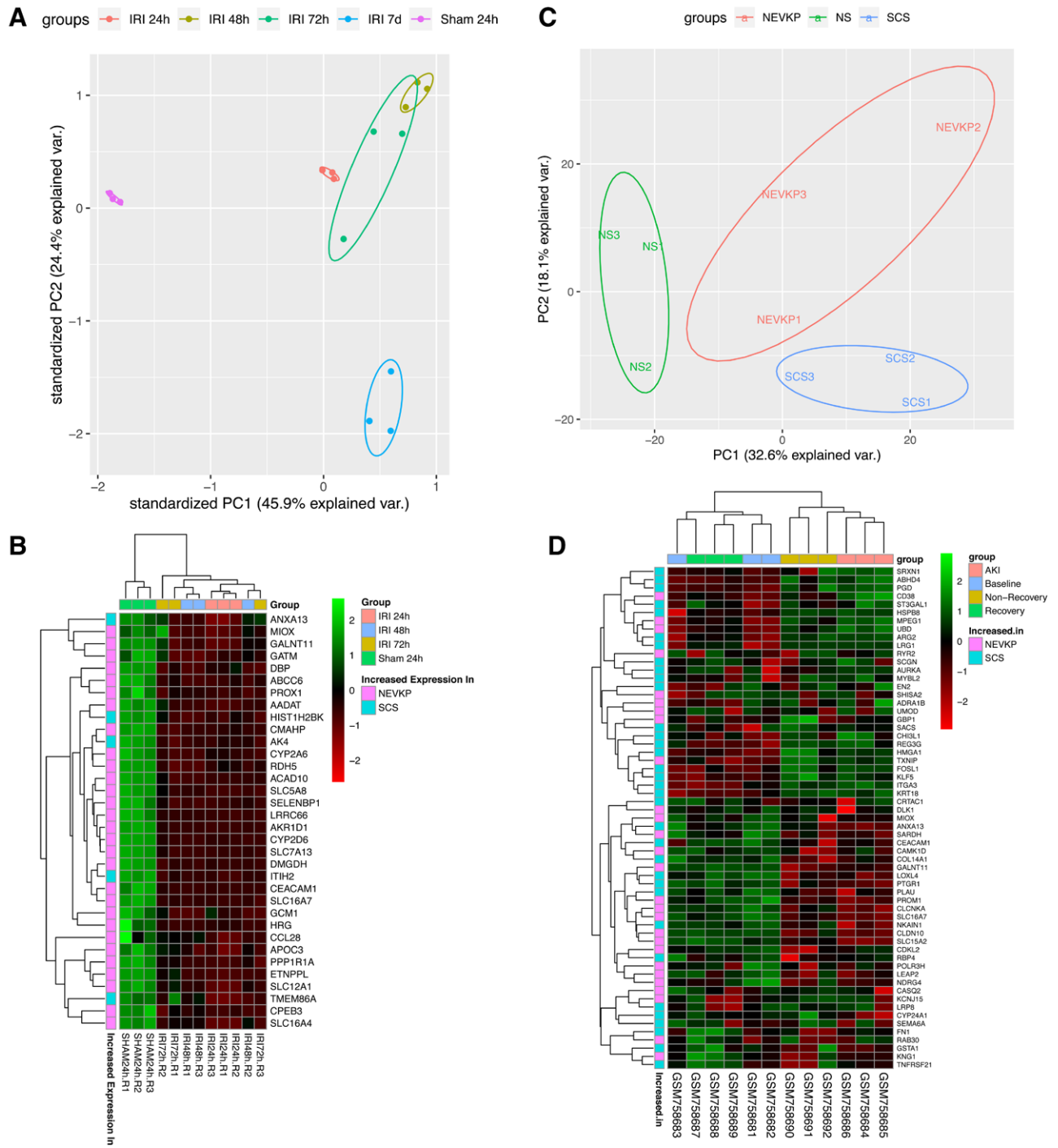

FIGURE 5. Validation of findings in relevant external data sets. A, GSEA-ranked genes show dynamic change across early time points following IRI 185 GSEA-ranked genes that overlapped with genes found DE in mice following IRI.[26] We examined the expression of these 185 genes in the murine data set in sham-operated mice and mice at early time points post-IRI. PC analysis was used to examine separation between the groups of mice at the various time points shown. The percent of the variability described by PCs 1 and 2 is indicated on the x-axis and y-axis, respectively. B, NEVKP profile demonstrates preserved expression of genes downregulated following IRI in a murine data set. Heatmap showing expression of the genes identified to have significantly reduced expression following IRI in mice[26] with unsupervised hierarchical clustering analysis. Columns represent the samples (annotated by group at the top, listed individually at the bottom), and rows represent the genes, with relative expression of each gene across all samples demonstrated by pseudocolour scale ranging from −2.5 (red = lower expression) to +2.5 (green = higher expression). Annotation of the rows denotes increased expression of the gene in NEVKP or SCS, respectively, in our microarray. C, IRI-associated genes in mouse confirm complete separation in phenotype in our data set. PC analysis of the DE genes from a mouse IRI data set[26] with orthologs in our microarray genes shows separation in the phenotypes represented in our study. The percent of the variability described by PCs 1 and 2 is indicated on the x-axis and y-axis, respectively. D, NEVKP-associated changes following IRI are relevant to the kidney's recovery from other forms of kidney injury. Heatmap showing the expression GSEA-ranked genes in a murine data set of a septic AKI with recovery and nonrecovery of renal function,[27] using unsupervised hierarchical clustering analysis. Columns represent the samples (annotated by group at the top, listed individually at the bottom) and rows represent the genes, with relative expression of each gene across all samples demonstrated by pseudocolour scale ranging from −3 (green = lower expression) to +3 (red = higher expression). AKI, acute kidney injury; DE, differential expression; IRI, ischemia-reperfusion injury; GSEA, gene set enrichment analysis; NEVKP, normothermic ex vivo kidney perfusion; NS, no storage; PC, principal component; SCS, static cold storage.

of identified orthologs from our GSEA-ranked gene list in the murine data set, in an unsupervised manner (Figure 5D). The differences in expression of our genes across the groups were sufficient to separate mice at baseline and with recovered renal function from those with AKI and those that did not recover renal function following resuscitation, suggesting that the reparative gene expression changes induced by NEVKP following IRI, are potentially relevant in other causes of AKI.

Internal Validation of Enriched Pathways Through Independent Confirmation of Differential Expression of Selected Representative Genes

Several representative genes were next chosen for internal validation, using an orthogonal method. Of the genes DE between NEVKP and SCS, we selected uromodulin (*umod*) and retinol-binding protein 4 (*rbp4*), which are associated with normal and injured kidneys, respectively. Consistent with our microarray findings, *umod* was significantly increased in NEVKP-treated kidneys compared with SCS-treated kidneys, and *rbp4* was significantly increased in SCS-treated kidneys in comparison with NEVKP-treated kidneys, using quantitative reverse-transcriptase polymerase chain reaction (Figure 6A and B). We next selected candidates from our GSEA-ranked genes to validate the differential regulation of specific pathways identified by that analysis. *mpc2* was chosen due to its involvement in key mitochondrial processes including pyruvate metabolism and the TCA cycle,[35] which were enriched in NEVKP kidneys. As predicted from GSEA ranking of genes, *mpc2* was significantly increased in NEVKP kidneys (Figure 6C). Finally, from the GSEA-ranked genes most highly correlating with NEVKP, we selected genes related to repair (*prom1/CD133*)[36] and preservation of renal function (*galnt11*)[37] in the kidney, in light of the superior function of NEVKP-treated kidneys despite an equal period of warm ischemia to SCS-treated kidneys. Consistent with

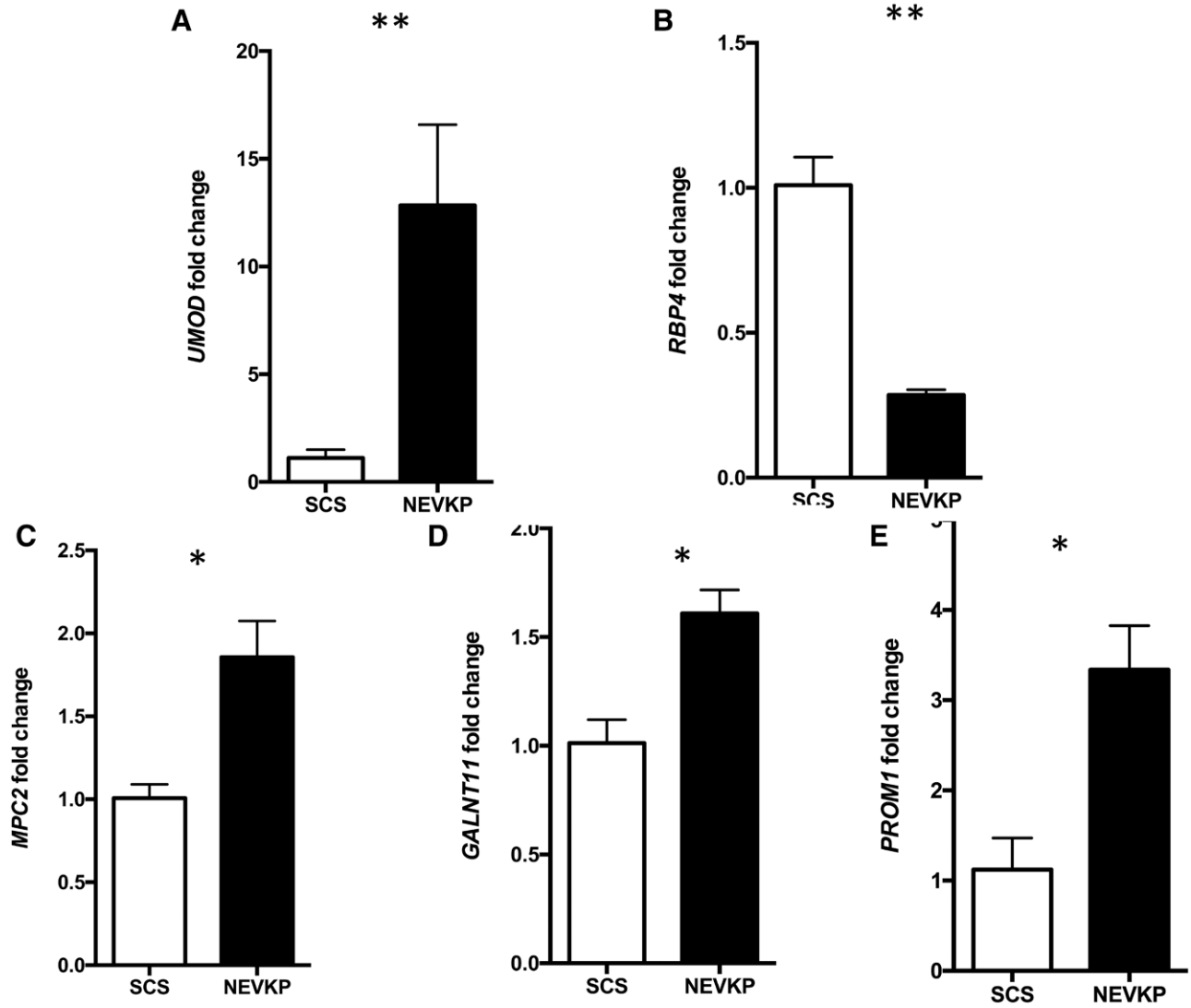

FIGURE 6. Internal validation of select genes of interest identified by differential expression analysis (A and B) or gene set enrichment analysis (C–E). A, *Umod*, (B) *Rbp4*, (C) *Mpc2*, (D) *Prom1*, and (E) *Galnt11*. Expression was assessed through quantitative reverse-transcriptase polymerase chain reaction and relative to Tbp1 that was used as the housekeeping gene. Expression is expressed as comparative threshold cycle (C_T) of the gene of interest subtracted by the C_T of the housekeeping gene for each sample with the median marked with a horizontal bar. *$P<0.05$, **$P<0.01$. NEVKP, normothermic ex vivo kidney perfusion; SCS, static cold storage.

the GSEA findings, these genes had significantly increased expression in NEVKP compared with SCS at mRNA level (Figure 6D and E).

DISCUSSION

Molecular mechanisms accounting for the superior posttransplantation DCD graft outcomes following NEVKP storage are unknown. This is the first study to use an unbiased, genome-wide transcriptome analysis to address this gap in understanding. Biopsies from POD3 kidneys were used to address this question as this represented the time point at which serum creatinine was most divergent between the NEVKP group and SCS group. Through this study, we have demonstrated that (1) gene expression of NEVKP kidneys is not significantly different from NS kidneys; (2) NEVKP kidneys demonstrate enrichment of fatty acid oxidation, TCA cycle, and oxidative phosphorylation, whereas SCS kidneys show enrichment of cell cycle and profibrotic ECM genes; (3) NEVKP restores the expression profile of genes commonly dysregulated following IRI and other forms of AKI, as evidenced by our analysis of relevant published data sets.

We first demonstrated that NEVKP storage resulted in a gene expression profile that was not significantly different from NS kidneys, which are spared additional ischemic damage from prolonged storage. The pathways and processes enriched in both NS and NEVKP when separately compared with SCS shared a striking overlap, emphasizing the similarities in their respective phenotypes.

In contrast, significant differences were noted between SCS-stored kidneys and NS kidneys. SCS-enriched pathways included those related to the inflammatory response (eg, IL-4, IL-13, and IL-10 signaling, beta-catenin signaling in T cells). The Notch developmental signaling pathway (enriched in SCS) has been implicated in peripheral T-cell differentiation,[38] renal repair following IRI,[39] and pathogenesis of renal fibrosis.[40-42] Organization of the ECM as occurs in the development of tubulointerstitial fibrosis[43,44] was also associated with SCS.

The pathways with reduced representation in SCS, as compared with NS, reflected key pathways of normal renal metabolism (fatty acid β-oxidation pathways[34]) and tubular function (SLC-mediated transmembrane transport, transport of small molecules), as previously described following IRI.[26]

Further supporting the idea that NEVKP induces a less damaged phenotype similar to NS kidneys, *Umod* expression was higher following NEVKP. Uromodulin, produced exclusively by tubular epithelial cells, is highly abundant in normal kidneys and released into both blood and urine.[29,45] Among its diverse roles, uromodulin has been shown to offer protection against IRI, to regulate the innate immune response in the kidney, and has been proposed as a biomarker of tubular health.[29,46-48] In contrast, RBP4 has been proposed as a biomarker of tubular injury.[49-51] Increased serum levels have been associated with CKD and increased urinary levels have been associated with AKI and impaired proximal tubular cell function.[52-54] Increased expression of RBP4 (as seen in SCS-treated grafts) is also reported in AKI posttransplant in human subjects.[55]

Subsequent pathway analysis demonstrated an important role for preserved mitochondrial metabolism in the NEVKP phenotype. The kidneys are highly metabolically active,[56] with a high requirement for ATP to achieve active solute transport. Thus, normal kidney function is tightly linked with mitochondrial energy production.[34,57-59] Fatty acid oxidation and the TCA cycle are the key mitochondrial pathways that supply energy precursors for oxidative phosphorylation in the kidney.[34,60] Pyruvate is a key intermediary in these pathways.[61,62] The *mpc2* gene encodes a protein responsible for the entry of pyruvate into the mitochondria and was confirmed to be significantly increased in NEVKP kidneys.[63]

These findings indicate that the maintenance of aerobic mitochondrial metabolism may be an important mechanism for improved graft function following NEVKP storage.

Inflammatory pathways identified in POD3 NEVKP-stored grafts were unexpected; however, inflammation is a critical feature of tissue repair and regeneration.[64] Indeed, impaired wound healing is reported in a mouse IFN-γ knockout model in keeping with the well-described antifibrotic properties of IFN-γ, which may also be advantageous in improving long-term graft function.[65] IFN-γ can also promote immunoregulation through the induction of indoleamine 2,3-dioxygenase in mesenchymal stem cells that then suppress T-cell proliferation.[66] Similarly, IL-12 inhibition through IFN-α can suppress T-cell proliferation.[67]

GSEA pathways in SCS-stored DCD grafts profile the early response to injury. Processes relating to altered transcription and translation formed a dominant cluster on the SCS-enrichment map (Figure 4B) as seen in the early transcriptional response in both mouse and human kidneys following IRI.[26,68-70] Likewise, the enriched terms relating to histone modification,[71] nuclear division, and DNA replication[68] are well described in the context of IRI.

SCS grafts were also enriched for pathways related to mitosis and for related terms on GO enrichment map clusters, including nuclear division, DNA replication, cell cycle checkpoints, and mitotic spindles; alterations to all of which have been previously described following IRI.[68,71] Moreover, E2F transcription factor-related gene sets, known to transcriptionally regulate many cell cycle genes,[31,32] were increased in SCS. Similar changes are initiated within hours of IRI in rodent models.[26] The transition from the premitotic G2-phase to the mitotic M-phase is necessary for cell division to replace damaged cells in tissue.[72] Although these pathways may also reflect increased division of infiltrating leukocytes, the simultaneous enrichment of myc oncogene-associated pathways suggests a component of tissue regeneration.[73] Alternatively, these terms may reflect cell cycle arrest that occurs following IRI, potentially mediating kidney fibrosis after injury through upregulated profibrotic cytokine production.[26,30,74,75] In support of this, additional processes linked with wound healing and the development of fibrosis also emerge on the SCS-enrichment map, namely ECM organization, integrin signaling, and cadherin binding.[43,76] Though initially reparative, processes observed in SCS such as wound healing responses, ECM organization, and cell cycle disturbance are clearly linked to the development of tubulointerstitial fibrosis.[74] Though the precise pathways underpinning the development of CKD following an episode of AKI remain unclear, maladaptive repair of injured tubules after AKI may promote this transition.[26,77,78]

Finally, by comparing the transcriptome of these grafts to a data set generated from a mouse IRI model, we demonstrated that IRI signals are mitigated following NEVKP. Although the transcriptome of the SCS group resembled that of murine kidneys after IRI, the transcriptome profile of NEVKP-treated

kidneys most resembled that of sham-operated mice.[26] Intriguingly, gene expression changes associated with the NEVKP phenotype are also observed in kidneys recovering from other types of AKI, underscoring their relevance to reparative pathways within the kidney.[27]

The genes and pathways governing repair in the kidney remain enigmatic; however, *prom1*, which showed increased expression in NEVKP-treated kidneys, has been proposed as a marker of a regenerative population of proximal tubular cells.[36,79-82] Increased numbers of PROM1/CD133-positive cells are seen in the kidneys and urine of transplant recipients as DGF recovers and may protect from IRI.[83-85] *Galnt11* is a member of a family of genes that mediate the *o*-glycosylation of various targets including mucin family members in the kidney that play roles in cell adhesion and signaling.[86-88] GALNT11 also glycosylates the endocytic receptor megalin, with impairment of proximal tubular cell function noted in *Galnt11*-deficient mice.[37] Furthermore, single-nucleotide polymorphisms at *GALNT11* and *UMOD* loci were significantly associated with declining renal function in a large genome-wide association study.[89]

The findings from this work have also been supported through high-throughput analyses in different models. Hameed et al[90] demonstrated an increase in transcripts related to stress and inflammatory pathways using discarded human kidneys that underwent 1 h of warm perfusion following cold storage compared with cold storage only. Oxidative phosphorylation was also identified as a key upregulated metabolic pathway through RNA sequencing and GSEA of discarded human kidney pairs subjected to 2 h of NEVKP versus cold storage in the work by Ferdinand et al.[91] Consistent with our study, induction of inflammatory pathway-related genes was also identified by this group. Subsequent removal of these mediators through hemoadsorption filters during NEVKP by this group did not improve perfusion parameters, but the effects of the removal of inflammatory molecules were not assessed in a survival model, and this strategy may remove mediators necessary for graft repair.[91] Conversely, work in liver transplant recipients demonstrated a decrease in inflammatory pathways; however, this difference may be explained by the effects of warm perfusion on a different organ system.[92] Complementing our studies, transcriptome analysis of lungs that were evaluated and deemed fit for transplantation through warm perfusion demonstrated an increase in transcripts of mitochondrial pathways, including oxidative phosphorylation, compared with grafts that were declined.[93] Adding to these previous studies, the work presented here is the first to demonstrate the reported pathways in a reproducible and clinically relevant animal survival model of kidney transplantation.

This transcriptome analysis identified candidate pathways for superiority of NEVKP, but some important limitations must be acknowledged. Transcript expression does not necessarily correlate with protein expression. Moreover, different processes may predominate at different time points during storage and at different locations throughout the kidney. Likewise, differences between NEVKP and hypothermic machine perfusion with or without oxygen are of interest. Technical considerations also impacted this study. The lack of an acceptable immunosuppressive protocol in porcine renal transplants limited the ability to assess the impact of NEVKP in allogeneic conditions. This likely has important consequences on the generalizability of the data as the potential role of inflammatory pathways identified following NEVKP storage may be altered or hampered in an immunosuppressed environment. Immunosuppressants and allogeneic conditions themselves may also provide different stimuli in either storage conditions promoting the role of other unidentified pathways that this analysis did not discover. Similarly, important pathways may not be identified because the number of analyzed samples was low due to the complexity and resource demands of this model. Nevertheless, our results are compelling, and the gene sets identified were cross-validated in 2 external data sets from a different species, suggesting generalizability of our findings.

In conclusion, this work highlights a key role for the enhancement of mitochondrial metabolism in abrogating IRI following NEVKP storage of DCD kidney grafts, likely accounting for the improved postoperative functioning. These findings contribute to a more comprehensive understanding of the mechanisms involved in promoting the improved renal function demonstrated after NEVKP storage.

Data Sharing Statement

The data discussed in this publication have been deposited to the gene expression omnibus database (www.ncbi.nlm.nih.gov/geo/) and are accessible through the number: GSE155418.

ACKNOWLEDGMENTS

The authors thank XVIVO Perfusion Inc. (Goteborg, Sweden) for their support. They highly appreciate the support of the John David and Signy Eaton Foundation. They also thank the Canadian Donation and Transplantation Research Program for their collaboration in this project.

REFERENCES

1. Hart A, Smith JM, Skeans MA, et al. OPTN/SRTR 2016 annual data report: kidney. *Am J Transplant.* 2018;18:18–113.
2. Israni AK, Zaun D, Bolch C, et al. OPTN/SRTR 2015 annual data report: deceased organ donation. *Am J Transplant.* 2017;17:503–542.
3. Cho YW, Terasaki PI, Cecka JM, et al. Transplantation of kidneys from donors whose hearts have stopped beating. *N Engl J Med.* 1998;338:221–225.
4. Alonso A, Fernández-Rivera C, Villaverde P, et al. Renal transplantation from non-heart-beating donors: a single-center 10-year experience. *Transplant Proc.* 2005;37:3658–3660.
5. Summers DM, Watson CJE, Pettigrew GJ, et al. Kidney donation after circulatory death (DCD): state of the art. *Kidney Int.* 2015;88:241–249.
6. Chapman J, Bock A, Dussol B, et al. Follow-up after renal transplantation with organs from donors after cardiac death. *Transpl Int.* 2006;19:715–719.
7. Tapiawala SN, Tinckam KJ, Cardella CJ, et al. Delayed graft function and the risk for death with a functioning graft. *J Am Soc Nephrol.* 2010;21:153–161.
8. Salazar Meira F, Zemiacki J, Figueiredo AE, et al. Factors associated with delayed graft function and their influence on outcomes of kidney transplantation. *Transplant Proc.* 2016;48:2267–2271.
9. Kaths JM, Echeverri J, Chun YM, et al. Continuous normothermic ex vivo kidney perfusion improves graft function in donation after circulatory death pig kidney transplantation. *Transplantation.* 2017;101:754–763.
10. Hamar M, Urbanellis P, Kaths MJ, et al. Normothermic ex vivo kidney perfusion reduces warm ischemic injury of porcine kidney grafts retrieved after circulatory death. *Transplantation.* 2018;102:1262–1270.
11. Zhao H, Alam A, Soo AP, et al. Ischemia-reperfusion injury reduces long term renal graft survival: mechanism and beyond. *Ebiomedicine.* 2018;28:31–42.

12. Kaths JM, Spetzler VN, Goldaracena N, et al. Normothermic ex vivo kidney perfusion for the preservation of kidney grafts prior to transplantation. *J Vis Exp.* 2015:e52909.
13. Gentleman RC, Carey VJ, Bates DM, et al. Bioconductor: open software development for computational biology and bioinformatics. *Genome Biol.* 2004;5:R80.
14. Irizarry RA, Bolstad BM, Collin F, et al. Summaries of Affymetrix GeneChip probe level data. *Nucleic Acids Res.* 2003;31:e15.
15. Carvalho BS, Irizarry RA. A framework for oligonucleotide microarray preprocessing. *Bioinformatics.* 2010;26:2363–2367.
16. Miller JA, Cai C, Langfelder P, et al. Strategies for aggregating gene expression data: the collapseRows R function. *BMC Bioinformatics.* 2011;12:322.
17. Bourgon R, Gentleman R, Huber W. Independent filtering increases detection power for high-throughput experiments. *Proc Natl Acad Sci U S A.* 2010;107:9546–9551.
18. Ritchie ME, Phipson B, Wu D, et al. limma powers differential expression analyses for RNA-sequencing and microarray studies. *Nucleic Acids Res.* 2015;43:e47.
19. Liu G, Loraine AE, Shigeta R, et al. NetAffx: Affymetrix probesets and annotations. *Nucleic Acids Res.* 2003;31:82–86.
20. Reimand J, Kull M, Peterson H, et al. g:Profiler—a web-based toolset for functional profiling of gene lists from large-scale experiments. *Nucleic Acids Res.* 2007;35:W193–W200.
21. Subramanian A, Tamayo P, Mootha VK, et al. Gene set enrichment analysis: a knowledge-based approach for interpreting genome-wide expression profiles. *Proc Natl Acad Sci U S A.* 2005;102:15545–15550.
22. Shannon P, Markiel A, Ozier O, et al. Cytoscape: a software environment for integrated models of biomolecular interaction networks. *Genome Res.* 2003;13:2498–2504.
23. Merico D, Isserlin R, Stueker O, et al. Enrichment map: a network-based method for gene-set enrichment visualization and interpretation. *PLoS One.* 2010;5:e13984.
24. Reimand J, Isserlin R, Voisin V, et al. Pathway enrichment analysis and visualization of omics data using g:Profiler, GSEA, Cytoscape and EnrichmentMap. *Nat Protoc.* 2019;14:482–517.
25. Kucera M, Isserlin R, Arkhangorodsky A, et al. AutoAnnotate: a cytoscape app for summarizing networks with semantic annotations. *F1000Res.* 2016;5:1717.
26. Liu J, Kumar S, Dolzhenko E, et al. Molecular characterization of the transition from acute to chronic kidney injury following ischemia/reperfusion. *JCI Insight*. 2017;2:e94716.
27. Tran M, Tam D, Bardia A, et al. PGC-1α promotes recovery after acute kidney injury during systemic inflammation in mice. *J Clin Invest.* 2011;121:4003–4014.
28. Nygard AB, Jørgensen CB, Cirera S, et al. Selection of reference genes for gene expression studies in pig tissues using SYBR green qPCR. *BMC Mol Biol.* 2007;8:67.
29. Devuyst O, Olinger E, Rampoldi L. Uromodulin: from physiology to rare and complex kidney disorders. *Nat Rev Nephrol.* 2017;13:525–544.
30. Moonen L, D'Haese PC, Vervaet BA. Epithelial cell cycle behaviour in the injured kidney. *Int J Mol Sci.* 2018;19:E2038.
31. Zhu W, Giangrande PH, Nevins JR. E2Fs link the control of G1/S and G2/M transcription. *EMBO J.* 2004;23:4615–4626.
32. Thurlings I, de Bruin A. E2F transcription factors control the roller coaster ride of cell cycle gene expression. *Methods Mol Biol.* 2016;1342:71–88.
33. Liberzon A, Birger C, Thorvaldsdóttir H, et al. The molecular signatures database (MSigDB) hallmark gene set collection. *Cell Syst.* 2015;1:417–425.
34. Kang HM, Ahn SH, Choi P, et al. Defective fatty acid oxidation in renal tubular epithelial cells has a key role in kidney fibrosis development. *Nat Med.* 2015;21:37–46.
35. Bender T, Martinou JC. The mitochondrial pyruvate carrier in health and disease: to carry or not to carry? *Biochim Biophys Acta.* 2016;1863:2436–2442.
36. Brossa A, Papadimitriou E, Collino F, et al. Role of CD133 molecule in Wnt response and renal repair. *Stem Cells Transl Med.* 2018;7:283–294.
37. Tian E, Wang S, Zhang L, et al. Galnt11 regulates kidney function by glycosylating the endocytosis receptor megalin to modulate ligand binding. *Proc Natl Acad Sci U S A.* 2019;116:25196–25202.
38. Osborne BA, Minter LM. Notch signalling during peripheral T-cell activation and differentiation. *Nat Rev Immunol.* 2007;7:64–75.
39. Kang HM, Huang S, Reidy K, et al. Sox9-positive progenitor cells play a key role in renal tubule epithelial regeneration in mice. *Cell Rep.* 2016;14:861–871.
40. Huang R, Zhou Q, Veeraragoo P, et al. Notch2/Hes-1 pathway plays an important role in renal ischemia and reperfusion injury-associated inflammation and apoptosis and the γ-secretase inhibitor DAPT has a nephroprotective effect. *Ren Fail.* 2011;33:207–216.
41. Edeling M, Ragi G, Huang S, et al. Developmental signalling pathways in renal fibrosis: the roles of Notch, Wnt and Hedgehog. *Nat Rev Nephrol.* 2016;12:426–439.
42. Duan X, Qin G. Notch inhibitor mitigates renal ischemia-reperfusion injury in diabetic rats. *Mol Med Rep.* 2020;21:583–588.
43. Liu Y. Cellular and molecular mechanisms of renal fibrosis. *Nat Rev Nephrol.* 2011;7:684–696.
44. Mack M, Yanagita M. Origin of myofibroblasts and cellular events triggering fibrosis. *Kidney Int.* 2015;87:297–307.
45. Clark JZ, Chen L, Chou CL, et al. Representation and relative abundance of cell-type selective markers in whole-kidney RNA-Seq data. *Kidney Int.* 2019;95:787–796.
46. El-Achkar TM, McCracken R, Liu Y, et al. Tamm-Horsfall protein translocates to the basolateral domain of thick ascending limbs, interstitium, and circulation during recovery from acute kidney injury. *Am J Physiol Renal Physiol.* 2013;304:F1066–F1075.
47. Liu M, Wang Y, Wang F, et al. Interaction of uromodulin and complement factor H enhances C3b inactivation. *J Cell Mol Med.* 2016;20:1821–1828.
48. Darisipudi MN, Thomasova D, Mulay SR, et al. Uromodulin triggers IL-1β-dependent innate immunity via the NLRP3 inflammasome. *J Am Soc Nephrol.* 2012;23:1783–1789.
49. Gonzalez-Calero L, Martin-Lorenzo M, Ramos-Barron A, et al. Urinary kininogen-1 and retinol binding protein-4 respond to acute kidney injury: predictors of patient prognosis? *Sci Rep.* 2016;6:19667.
50. Klisic A, Kavaric N, Ninic A. Retinol-binding protein 4 versus albuminuria as predictors of estimated glomerular filtration rate decline in patients with type 2 diabetes. *J Res Med Sci.* 2018;23:44.
51. Musiał K, Zwolińska D. Fractional excretion as a new marker of tubular damage in children with chronic kidney disease. *Clin Chim Acta.* 2018;480:99–106.
52. Domingos MA, Moreira SR, Gomez L, et al. Urinary retinol-binding protein: relationship to renal function and cardiovascular risk factors in chronic kidney disease. *PLoS One.* 2016;11:e0162782.
53. Kocełak P, Owczarek A, Bożentowicz-Wikarek M, et al. Plasma concentration of retinol binding protein 4 (RBP4) in relation to nutritional status and kidney function in older population of PolSenior Study. *Adv Med Sci.* 2018;63:323–328.
54. Norden AG, Lapsley M, Unwin RJ. Urine retinol-binding protein 4: a functional biomarker of the proximal renal tubule. *Adv Clin Chem.* 2014;63:85–122.
55. Famulski KS, de Freitas DG, Kreepala C, et al. Molecular phenotypes of acute kidney injury in kidney transplants. *J Am Soc Nephrol.* 2012;23:948–958.
56. Pagliarini DJ, Calvo SE, Chang B, et al. A mitochondrial protein compendium elucidates complex I disease biology. *Cell.* 2008;134:112–123.
57. Forbes JM, Thorburn DR. Mitochondrial dysfunction in diabetic kidney disease. *Nat Rev Nephrol.* 2018;14:291–312.
58. Ralto KM, Parikh SM. Mitochondria in acute kidney injury. *Semin Nephrol.* 2016;36:8–16.
59. Brooks C, Wei Q, Cho SG, et al. Regulation of mitochondrial dynamics in acute kidney injury in cell culture and rodent models. *J Clin Invest.* 2009;119:1275–1285.
60. Jassem W, Fuggle SV, Rela M, et al. The role of mitochondria in ischemia/reperfusion injury. *Transplantation.* 2002;73:493–499.
61. McCommis KS, Finck BN. Mitochondrial pyruvate transport: a historical perspective and future research directions. *Biochem J.* 2015;466:443–454.
62. Shi L, Tu BP. Acetyl-CoA and the regulation of metabolism: mechanisms and consequences. *Curr Opin Cell Biol.* 2015;33:125–131.
63. Gansemer ER, McCommis KS, Martino M, et al. NADPH and glutathione redox link TCA cycle activity to endoplasmic reticulum homeostasis. *iScience.* 2020;23:101116.
64. Serhan CN, Chiang N, Dalli J. The resolution code of acute inflammation: novel pro-resolving lipid mediators in resolution. *Semin Immunol.* 2015;27:200–215.
65. Kanno E, Tanno H, Masaki A, et al. Defect of interferon γ leads to impaired wound healing through prolonged neutrophilic inflammatory response and enhanced MMP-2 activation. *Int J Mol Sci.* 2019;20:E5657.

66. Zimmermann JA, Hettiaratchi MH, McDevitt TC. Enhanced immunosuppression of T cells by sustained presentation of bioactive interferon-γ within three-dimensional mesenchymal stem cell constructs. *Stem Cells Transl Med.* 2017;6:223–237.
67. Mehrotra A, D'Angelo JA, Romney-Vanterpool A, et al. IFN-alpha suppresses myeloid cytokine production, impairing IL-12 production and the ability to support T cell proliferation. *J Infect Dis*. 2020;222:148–157.
68. Damman J, Bloks VW, Daha MR, et al. Hypoxia and complement-and-coagulation pathways in the deceased organ donor as the major target for intervention to improve renal allograft outcome. *Transplantation.* 2015;99:1293–1300.
69. Giraud S, Steichen C, Allain G, et al. Dynamic transcriptomic analysis of ischemic injury in a porcine pre-clinical model mimicking donors deceased after circulatory death. *Sci Rep.* 2018;8:5986.
70. Johnsen M, Kubacki T, Yeroslaviz A, et al. The integrated RNA landscape of renal preconditioning against ischemia-reperfusion injury. *J Am Soc Nephrol.* 2020;31:716–730.
71. Guo C, Dong G, Liang X, et al. Epigenetic regulation in AKI and kidney repair: mechanisms and therapeutic implications. *Nat Rev Nephrol.* 2019;15:220–239.
72. Krafts KP. Tissue repair: the hidden drama. *Organogenesis.* 2010;6:225–233.
73. Dang CV. c-Myc target genes involved in cell growth, apoptosis, and metabolism. *Mol Cell Biol.* 1999;19:1–11.
74. Yang L, Besschetnova TY, Brooks CR, et al. Epithelial cell cycle arrest in G2/M mediates kidney fibrosis after injury. *Nat Med.* 2010;16:535–543.
75. Kishi S, Brooks CR, Taguchi K, et al. Proximal tubule ATR regulates DNA repair to prevent maladaptive renal injury responses. *J Clin Invest.* 2019;129:4797–4816.
76. Henderson NC, Sheppard D. Integrin-mediated regulation of TGFβ in fibrosis. *Biochim Biophys Acta.* 2013;1832:891–896.
77. Liu BC, Tang TT, Lv LL, et al. Renal tubule injury: a driving force toward chronic kidney disease. *Kidney Int.* 2018;93:568–579.
78. Ferenbach DA, Bonventre JV. Mechanisms of maladaptive repair after AKI leading to accelerated kidney ageing and CKD. *Nat Rev Nephrol.* 2015;11:264–276.
79. Kramann R, Kusaba T, Humphreys BD. Who regenerates the kidney tubule? *Nephrol Dial Transplant.* 2015;30:903–910.
80. Takaori K, Yanagita M. Kidney regeneration and stem cells. *Anat Rec (Hoboken).* 2014;297:129–136.
81. Sallustio F, Serino G, Schena FP. Potential reparative role of resident adult renal stem/progenitor cells in acute kidney injury. *Biores Open Access.* 2015;4:326–333.
82. Aggarwal S, Grange C, Iampietro C, et al. Human CD133+ renal progenitor cells induce erythropoietin production and limit fibrosis after acute tubular injury. *Sci Rep.* 2016;6:37270.
83. Loverre A, Capobianco C, Ditonno P, et al. Increase of proliferating renal progenitor cells in acute tubular necrosis underlying delayed graft function. *Transplantation.* 2008;85:1112–1119.
84. Dimuccio V, Ranghino A, Praticò Barbato L, et al. Urinary CD133+ extracellular vesicles are decreased in kidney transplanted patients with slow graft function and vascular damage. *PLoS One.* 2014;9:e104490.
85. Li X, Wan Q, Min J, et al. Premobilization of CD133+ cells by granulocyte colony- stimulating factor attenuates ischemic acute kidney injury induced by cardiopulmonary bypass. *Sci Rep.* 2019;9:2470.
86. Boskovski MT, Yuan S, Pedersen NB, et al. The heterotaxy gene GALNT11 glycosylates Notch to orchestrate cilia type and laterality. *Nature.* 2013;504:456–459.
87. Leroy X, Copin MC, Devisme L, et al. Expression of human mucin genes in normal kidney and renal cell carcinoma. *Histopathology.* 2002;40:450–457.
88. Hanisch FG, Reis CA, Clausen H, et al. Evidence for glycosylation-dependent activities of polypeptide N-acetylgalactosaminyltransferases rGalNAc-T2 and -T4 on mucin glycopeptides. *Glycobiology.* 2001;11:731–740.
89. Gorski M, Tin A, Garnaas M, et al. Genome-wide association study of kidney function decline in individuals of European descent. *Kidney Int.* 2015;87:1017–1029.
90. Hameed AM, Lu DB, Patrick E, et al. Brief normothermic machine perfusion rejuvenates discarded human kidneys. *Transplant Direct.* 2019;5:e502.
91. Ferdinand JR, Hosgood SA, Moore T, et al. Cytokine absorption during human kidney perfusion reduces delayed graft function-associated inflammatory gene signature. *Am J Transplant*. [Epub ahead of print. October 23, 2020]. doi:10.1111/ajt.16371
92. Jassem W, Xystrakis E, Ghnewa YG, et al. Normothermic machine perfusion (NMP) inhibits proinflammatory responses in the liver and promotes regeneration. *Hepatology.* 2019;70:682–695.
93. Ferdinand JR, Morrison MI, Andreasson A, et al. Transcriptional analysis identifies novel biomarkers associated with successful ex-vivo perfusion of human donor lungs. *bioRxiv*. Preprint. Posted online April 17, 2019. doi: 10.1101/612374.